Reductive Isopropyl Radical Elimination from (dpp-bian)Mg-*i*Pr(Et_2O)

Igor L. Fedushkin*[a] **Alexandra A. Skatova,**[a] **Markus Hummert,**[b] **and Herbert Schumann***[b]

Dedicated to Prof. Dr. Sergei F. Zhiltsov on the occasion of his 70th birthday

Keywords: Magnesium / N ligands / Alkyl complexes / Reductive elimination

The reaction of (dpp-bian)Na(Et_2O) with one equiv. of *i*PrMgCl in hexane affords (dpp-bian)Mg-*i*Pr(Et_2O) (**1**) whereas (dpp-bian)Mg(Et_2O)$_2$ (**2**) is formed when this reaction is carried out in Et_2O as a result of *isopropyl* radical elimination. Compound **1** which is stable in hexane and Et_2O also decomposes in THF with elimination of *isopropyl* radicals yielding (dpp-bian)Mg(THF)$_2$. The reaction of (dpp-bian)Na$_2$(Et_2O)$_3$ with two equiv. of *i*PrMgCl in Et_2O produces **2** and *i*Pr$_2$Mg, which then interact to give (dpp-bian)(Mg-*i*Pr)$_2$(Et_2O) (**3**) when treated with hexane or toluene. Compounds **1**–**3** were characterized by elemental analysis, UV/Vis and NMR spectroscopy, as well as by single-crystal X-ray diffraction.
(© Wiley-VCH Verlag GmbH & Co. KGaA, 69451 Weinheim, Germany, 2005)

Introduction

Grignard compounds[1] are one of the most useful reagents in organic and organometallic chemistry.[2] Several decades after the discovery of these highly reactive species, it has turned out that the substitution of the halogen atom in alkyl- or arylmagnesium halides by other functional groups may strongly affect the reactivity, structure, and solution behavior of such organomagnesium compounds. The first alkylmagnesium amide, *i*PrMgNPh$_2$(Et_2O)$_2$ was synthesized in 1967,[3a] and already two years later, X-ray diffraction data of e.g. $\{[Me_2N(CH_2)_2MeN]MgMe\}_2$ were published.[3b] Recently, a series of heteroleptic alkyl- and alkynylmagnesium amides have been prepared.[3c] A new period in organomagnesium chemistry started with the use of tris(pyrazolyl)borato[4] and ketiminato ligands[5] which allowed the synthesis of monomeric, low-coordinate magnesiumalkyls.

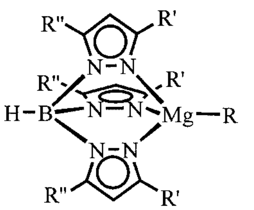

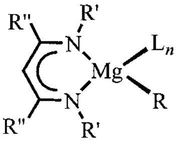

L = coordinating solvent; *n* = 0 or 1

R = alkyl or aryl; R' and R'' = H or alkyl

We have reported on the successful synthesis of main group metal complexes with anionic or radical-anionic species of the 1,2-bis{(2,6-diisopropylphenyl)imino}acenaphthene (dpp-bian) ligand e.g. $\{[M]^+_n[(\text{dpp-bian})]^{n-}(L)_x\}$ (M = Li, Na; *n* = 1–4; L = Et_2O, THF)[6a,6b] and $\{[M]^{2+}[(\text{dpp-bian})]^{2-}(THF)_x\}$ (M = Mg, Ca, Ge).[6c,6d,6e] Up to this time the aryl-bian system was mainly used in transition metal chemistry,[7] but we have demonstrated that the magnesium complex (dpp-bian)Mg(THF)$_3$ is also a powerful reagent in organic synthesis.[6e,8a,8b] Thus, the electron transfer from this complex to Ph_2CO affords the pinacol coupling product, while its reaction with 9-(10H)-anthracenone yields the antryloxymagnesium derivative.[8a]

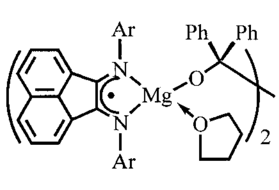

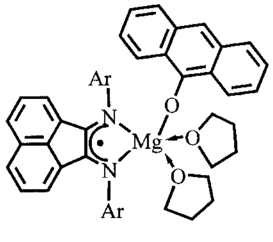

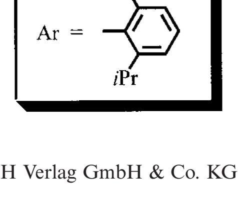

---

[a] G. A. Razuvaev Institute of Organometallic Chemistry of Russian Academy of Sciences,
Tropinina 49, 603950 Nizhny Novgorod GSP-445, Russia
Fax: +7-8312-661-497
E-mail: igorfed@imoc.sinn.ru
[b] Institut für Chemie der Technischen Universität Berlin,
Straße des 17. Juni 135, 10623 Berlin, Germany
Fax: +49-30-3142-2168
E-mail: schumann@chem.tu-berlin.de

DOI: 10.1002/ejic.200400973

A further interesting type of reaction of (dpp-bian)-Mg(THF)$_3$ is the oxidative addition of acidic substances such as phenylacetylene[8b] or enolizable ketones.[8b]

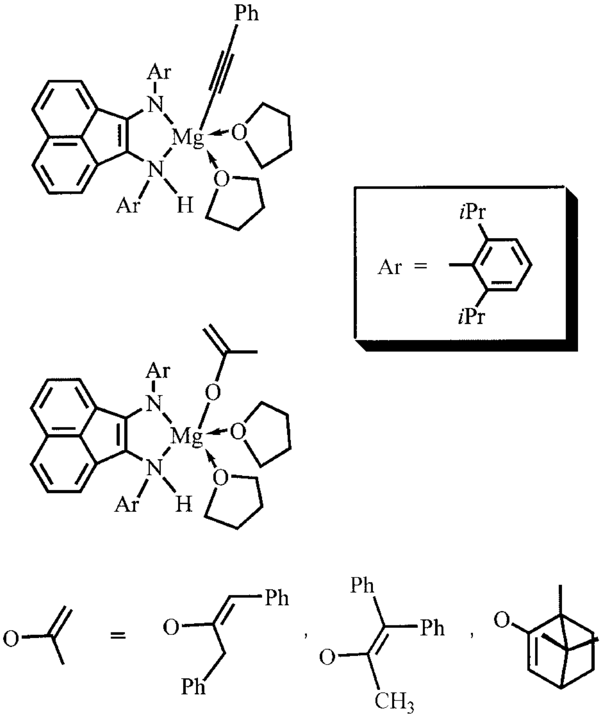

In this paper we report on the solvent induced radical elimination of the *isopropyl* group from (dpp-bian)Mg-*i*Pr-(Et$_2$O) (**1**) – a process that is possible due to the ability of the dpp-bian radical anion to be further reduced to the dianion.

Results and Discussion

Reaction of *i*PrMgCl with (dpp-bian)$^-$Na$^+$ and (dpp-bian)$^{2-}$Na$^+_2$ in Et$_2$O and Hexane

Exchange reactions of (dpp-bian)Na(Et$_2$O) with methyl- and ethylmagnesium bromide or trimethylsilylmethylmagnesium chloride in Et$_2$O produce cherry-red solutions from which the respective magnesiumalkyls, supported by the dpp-bian ligand, can be isolated as red crystalline substances in high yields.[8d] In contrast, the in situ reaction of (dpp-bian)Na(Et$_2$O) with one equiv. of *i*PrMgCl in Et$_2$O affords a green-brown solution from which yellowish-green crystals precipitate. As already indicated by the green color, which signals the presence of dpp-bian dianions, the expected (dpp-bian)Mg-*i*Pr(Et$_2$O) (**1**) containing (dpp-bian) radical anions is not formed. Accordingly, the isolated product (72% yield) proved to be (dpp-bian)Mg(Et$_2$O)$_2$ (**2**). The formation of **2** suggests that an intermediate formed in the course of the reaction obviously disproportionates with reduction of the dpp-bian radical anions to dianions and oxidation of the *isopropyl* carbanions to *isopropyl* radicals (Scheme 1). However, we succeeded in the synthesis of (dpp-bian)(Mg-*i*Pr)(Et$_2$O) (**1**), using hexane instead of Et$_2$O as the solvent in the reaction of (dpp-bian)Na with *i*PrMgCl. In this case, complex **1** can be isolated in yields up to 40% as blocklike, deep-red crystals along with 30 to 50% of **2** (Scheme 1).

In contrast to our expectations, **1** is stable in Et$_2$O, which means that an adduct of (dpp-bian)Na with *i*PrMgCl, formed initially in the reaction conducted in Et$_2$O, will disproportionate with elimination of *i*Pr radicals. But, according to ^{1}H NMR spectroscopic results, **1** disproportionates immediately with elimination of *i*Pr radicals when dissolved in THF.

The above suggested redox reaction and hence the elimination of *isopropyl* radicals should be excluded if the dpp-bian complex used in the reaction with *i*PrMgCl already contains the dpp-bian ligand in the dianionic form. Therefore, we reacted (dpp-bian)Na$_2$(Et$_2$O)$_2$ with two equiv. of *i*PrMgCl in Et$_2$O. The reaction results in an almost quantitative precipitation of **2** and, as a consequence, in the formation of Mg(*i*Pr)$_2$. Evaporation of the solvent from the entire reaction mixture followed by treatment of the remaining green solid components with toluene caused its dissolution at 70 °C yielding a deep-blue solution. Recrystallization of the solid remaining after removal of the toluene in vacuo, from hexane affords deep-blue crystals of (dpp-bian)(Mg-*i*Pr)$_2$(Et$_2$O) (**3**) with 60% yield (Scheme 2).

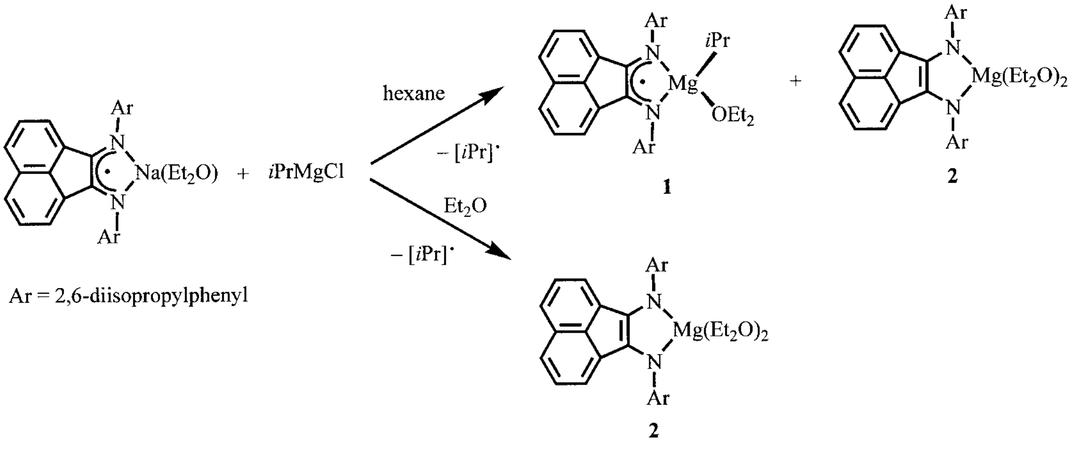

Scheme 1.

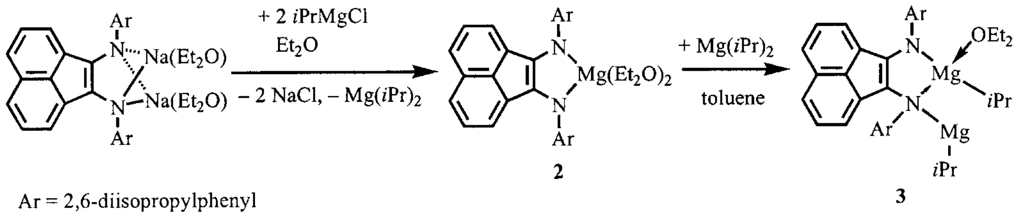

Scheme 2.

Since, according to X-ray crystal structure analysis, complex **3** consists of two *i*PrMg units, asymmetrically coordinated by the dpp-bian dianion, we have proved that the elimination of *i*Pr radicals is very much dependent on whether the coordinating ligand bound to magnesium can be reduced or not. At this point it should be noted, that magnesiumalkyls (alkyl = Me, *i*Pr, *t*Bu) supported by tris(pyrazolyl)borato[4] and ketiminato[5] ligands do not eliminate alkyl radicals because the monoanionic ketiminato and tris(pyrazolyl)borato ligands are not further to reduce.

Molecular Structures of 1, 2, and 3

The molecular structures of **1**, **2**, and **3** are depicted in Figure 1, Figure 2, and Figure 3, respectively. The crystal data collection and structure refinement data of **1**, **2**, and **3** are listed in Table 1, selected bond lengths and bond angles of the molecules are listed in Table 2. X-ray quality crystals were obtained from hexane (**1**) or toluene (**2**, **3**). The molecular structure of (dpp-bian)Mg(Et$_2$O)$_2$ (**2**) [Mg–N(1) 2.002, Mg–N(2) 2.003 Å] is very close to that of the analogous THF adduct (dpp-bian)Mg(THF)$_2$ [Mg–N(1) 1.994, Mg–N(2) 2.004 Å][6c] and will not be discussed in detail here.

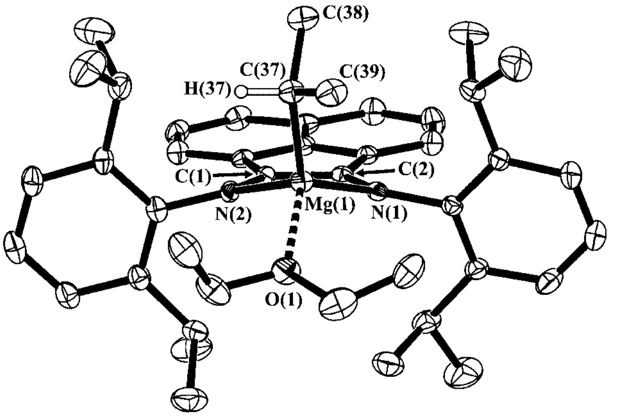

Figure 1. Molecular structure (ORTEP)[9] of **1**. The hydrogen atoms are omitted. Thermal ellipsoids are drawn at 30% probability level.

The unit cell of (dpp-bian)(Mg-*i*Pr)(Et$_2$O) (**1**) contains two independent molecules, the parameters of which are very much alike. Hence, the molecular structure of only one of them is depicted in Figure 1. Similar to (dpp-bian)Mg(Et$_2$O)$_2$ (**2**) the magnesium atom in **1** is four-coordinate. The radical anionic character of the dpp-bian ligand in **1** is indicated by the elongated Mg–N distances [Mg(1)–N(1) 2.120, Mg(1)–N(2) 2.103 Å] compared to those in **2** [Mg(1)–N(1) 2.002 and Mg(1)–N(2) 2.003 Å] containing the dianionic dpp-bian ligand. The Mg–O distance in **1** (2.051 Å) only slightly exceeds the Mg–O distances in **2** (2.009 and 2.049 Å). The Mg–C(37) bond length (2.145 Å) in **2** is comparable with the distance between Mg(2) and the methine

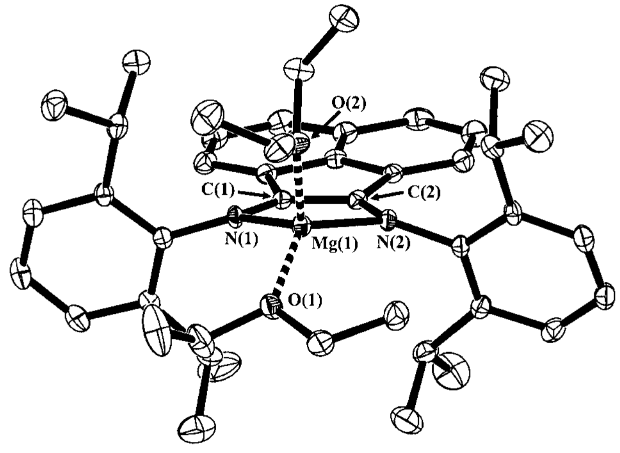

Figure 2. Molecular structure (ORTEP)[9] of **2**. The hydrogen atoms are omitted. Thermal ellipsoids are drawn at 30% probability level.

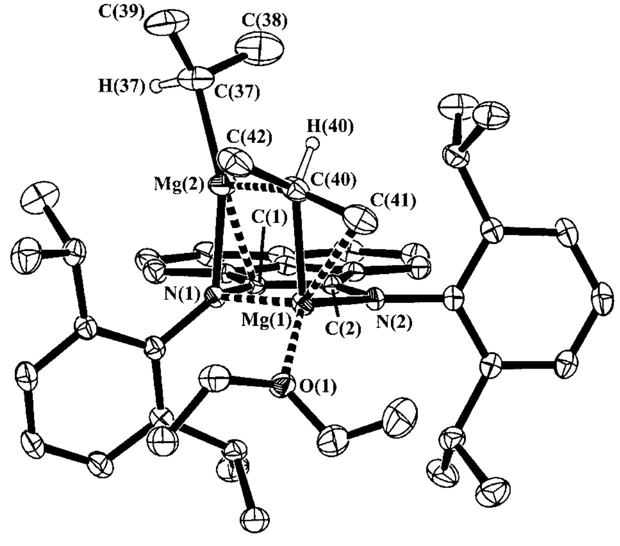

Figure 3. Molecular structure (ORTEP)[9] of **3**. The hydrogen atoms are omitted. Thermal ellipsoids are drawn at 30% probability level.

carbon atom C(37) of the terminal isopropyl group in **3** (2.129 Å).

In (dpp-bian)(Mg-*i*Pr)$_2$(Et$_2$O) (**3**), the coordinating sites of the two magnesium atoms relative to the dpp-bian ligand are quite different. The Mg(1) atom lies almost perfectly in the plane formed by the diimine fragment, whereas Mg(2) is positioned above this plane. At first sight, the molecular structure of **3** looks like that of a complex of (dpp-bian)-Mg(Et$_2$O)$_2$ (**2**) and *i*Pr$_2$Mg with the magnesium atom of the *i*Pr$_2$Mg unit (Mg(2)) being coordinated by the lone electron pair of N(1). However, the Mg(2)–C(37) bond length (2.129 Å) is much shorter than the Mg(2)–C(40) distance (2.282 Å), which in turn is somewhat longer than the Mg(1)–C(40) bond (2.266 Å). Further, taking into account, that the Mg(1)–N(1) and Mg(1)–N(2) bonds differ in their length (2.101 and 2.030 Å, respectively) and that the Mg(2)–N(1) distance (2.070 Å) is relatively short, it can be concluded that the Mg(1)–N(1) bond is a coordinative bond whereas the Mg(1)–N(2) bond is a covalent amido bond.

Table 2. Selected bond lengths [Å] and angles [°] for complexes **1**, **2**, and **3**.

Compound	1	2	3
C(1)–N(1)	1.331(4)	1.383(4)	1.440(3)
C(1)–C(2)	1.437(5)	1.395(5)	1.406(3)
C(1)–Mg(1)	2.793(4)	2.680(4)	
C(40)–Mg(1)			2.266(3)
C(40)–Mg(2)			2.282(4)
C(41)–Mg(1)			2.534(4)
C(37)–Mg(2)			2.129(3)
C(1)–Mg(2)			2.524(3)
C(2)–N(2)	1.332(4)	1.401(4)	1.368(3)
C(2)–Mg(1)	2.792(4)	2.684(4)	
C(37)–Mg(1)	2.145(4)		
N(1)–Mg(1)	2.120(3)	2.002(3)	2.101(2)
N(1)–Mg(2)			2.070(2)
N(2)–Mg(1)	2.103(3)	2.004(3),	2.030(2)
O(1)–Mg(1)	2.052(3)	2.009(2)	2.007(2)
O(2)–Mg(1)		2.049(3)	
Mg(1)–Mg(2)			2.7524(12)
Mg(1)–C(40)–Mg(2)			74.48(10)
Mg(2)–N(1)–Mg(1)			82.57(8)
O(1)–Mg(1)–N(2)	104.81(12)	128.82(12)	130.17(8)
O(1)–Mg(1)–N(1)	115.94(12)	112.11(11)	108.78(8)
N(1)–Mg(1)–N(2)	81.95(12)	90.27(12)	89.29(9)
N(1)–Mg(1)–O(2)		116.27(12)	
N(2)–Mg(1)–O(2)		113.94(11)	
O(1)–Mg(1)–O(2)		96.93(11)	
O(1)–Mg(1)–C(37)	107.05(14)		
N(2)–Mg(1)–C(37)	118.53(14)		
N(1)–Mg(1)–C(37)	125.26(14)		

UV/Vis and NMR Spectroscopic Studies on Solutions of 1 and 3

The solution behavior of **1** and **3** is quite remarkable. Both compounds are soluble in hexane and toluene and are stable in these solutions for several days. As already mentioned above, compound **1** is also stable in Et$_2$O, but disproportionates in THF while dissolution of **3** in Et$_2$O as well as in THF causes immediate decomposition into (dpp-bian) Mg(Et$_2$O)$_2$ and *i*Pr$_2$Mg.

The electron absorption spectra of solutions of **1** in Et$_2$O and of **3** in hexane and Et$_2$O are presented in Figure 4. The absorption maximum at 520 nm in the UV/Vis spectrum of **1** indicates the presence of dpp-bian radical anions. The absorption maximum at 598 nm in the spectrum of **3** in hexane corresponds to the dianion of dpp-bian, and the

Table 1. Crystal data and structure refinement details for **1**, **2** and **3**

Compound	(dpp-bian)Mg-*i*Pr(Et$_2$O) (**1**)	(dpp-bian)Mg(Et$_2$O)$_2$ (**2**)	(dpp-bian)(Mg-*i*Pr)$_2$(Et$_2$O) (**3**)
Empirical formula	$C_{43}H_{57}MgN_2O$	$C_{51}H_{68}MgN_2O_2$	$C_{46}H_{64}Mg_2N_2O$
Formula mass	624.24	765.38	709.64
Temperature [K]	173(2)	173(2)	173(2)
Crystal system	monoclinic	monoclinic	monoclinic
Space group	$P2_1/n$	$P2_1/n$	$P2_1/n$
Unit-cell dimensions	a = 22.0060(2), b = 17.27160(10), c = 22.2811(2) Å, β = 114.2780(10)°	a = 12.2200(2), b = 19.95660(10), c = 18.6465(2) Å, β = 92.7850(10)°	a = 10.839(1), b = 19.5844(2), c = 19.814(1) Å, β = 93.9550(10)°
Volume [Å^3]	7719.62(11)	4541.94(9)	4195.89(4)
Z	8	4	4
Density (calculated) [g/cm^3]	1.105	1.119	1.123
Absorption coefficient [mm^{-1}]	0.079	0.079	0.093
$F_{(000)}$	2792	1664	1544
Crystal size [mm^3]	0.50 × 0.30 × 0.24	0.40 × 0.28 × 0.12	0.88 × 0.30 × 0.20
θ range for data collection, [°]	1.02 to 25.00	1.50 to 24.00	1.46 to 25.00
Index ranges	$-23 \leq h \leq 26$, $-20 \leq k \leq 20$, $-26 \leq l \leq 26$	$-11 \leq h \leq 13$, $-21 \leq k \leq 22$, $-17 \leq l \leq 21$	$-12 \leq h \leq 12$, $-23 \leq k \leq 23$, $-23 \leq l \leq 15$
Reflections collected	45336	24977	25382
Independent reflections	13575 [R(int) = 0.1492]	7108 [R(int) = 0.1115]	7378 [R(int) = 0.0825]
Max./min. transmission	0.994655/0.650449	0.965465/0.506961	0.980072/0.47254
Data/restraints/parameters	13575/2/872	7108/0/518	7378/4/489
Goodness-of-fit on F^2	0.955	0.999	1.024
Final R indices [$I > 2\sigma(I)$]	$R1$ = 0.0724, $wR2$ = 0.1341	$R1$ = 0.0657, $wR2$ = 0.1307	$R1$ = 0.0598, $wR2$ = 0.1476
R indices (all data)	$R1$ = 0.1821, $wR2$ = 0.1728	$R1$ = 0.1436, $wR2$ = 0.1634	$R1$ = 0.1044, $wR2$ = 0.1661
Largest diff. peak and hole [e/Å^3]	0.300 and –0.310	0.252 and –0.341	0.381 and –0.398

absorption maximum at 737 nm in the spectrum of **3** in Et_2O indicates the formation of **2** by dismutation of **3** into (dpp-bian)Mg(Et_2O)$_2$ (**2**) and *i*Pr_2Mg. The latter compound is colorless and invisible in the UV/Vis spectrum.

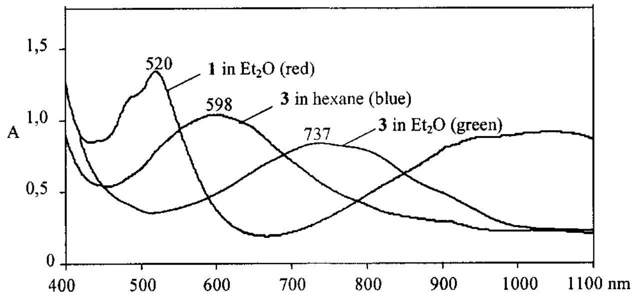

Figure 4. UV/Vis spectra of **1** and **3**.

The ^1H NMR spectrum of the blue solution of **3** in [D_8] toluene (Figure 5) reveals six septets, which are assigned to the methine protons of the *i*Pr substituents of the dpp-bian phenyl rings. The integrals of the two septets at δ = 3.69 and 3.54 ppm are five times higher than those of the other four very broad septets at 3.94, 3.80, 3.64 and 3.40 ppm and the overall integral of the six septets is twice as high as that of the multiplet at δ = 0.32 ppm, which is assigned to the methine protons of the isopropyl groups attached to the two magnesium atoms.

We conclude from these facts, that solutions of **3** in [D_8]-toluene contain two kinds of molecules differing in their structure. The major part consists of molecules in which Mg(2) is symmetrically positioned above the center of the metallocycle formed by the atoms C(1)–C(2)–N(1)–N(2)–Mg(1). Therefore, the signals of the two pairs of the *i*Pr methine protons substituting the phenyl rings and being situated above and below the diimine plane are different (3.69 and 3.54 ppm). A similar symmetrical structure has been found for (dpp-bian)(H)MgC≡CPh(THF)$_2$[8b] in THF solution, in which the cation H^+ is delocalized between the two nitrogen atoms. The minor part of the molecules, present in solution, possesses the structure established by crystal structure analysis, thus causing nonequivalence of all four phenyl ring substituting methine protons (3.94, 3.80, 3.64, and 3.40 ppm).

Going from toluene to THF as the solvent causes a dramatic change in the color of solution **3** (blue to green) as well as the appearance of the ^1H NMR spectrum (Figure 6).

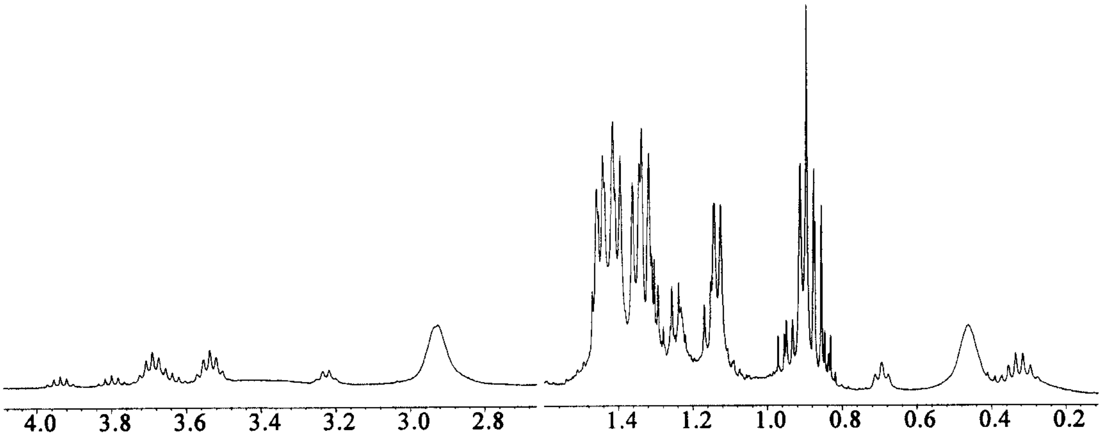

Figure 5. ^1H NMR spectrum of **3** in [D_8]toluene (400 MHz, 294 K). The aromatic region is omitted.

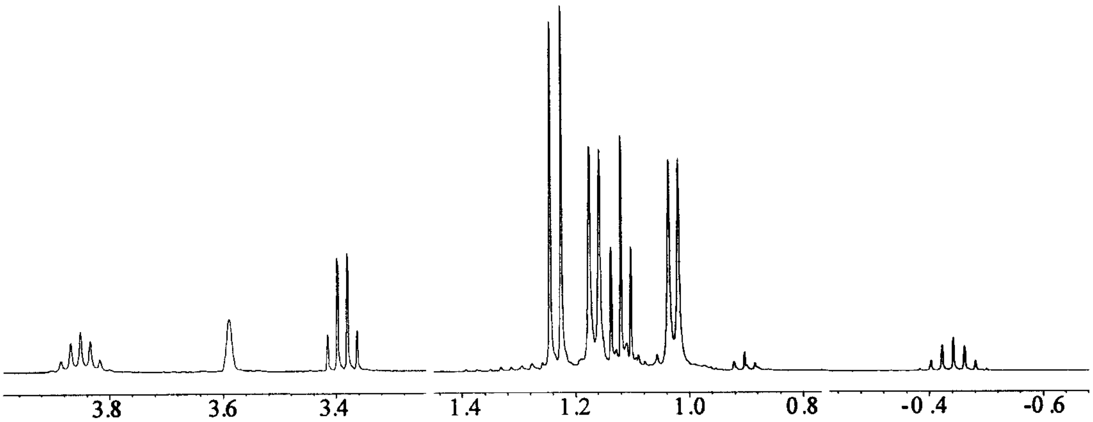

Figure 6. ^1H NMR spectrum of **3** in [D_8]THF (400 MHz, 294 K). The aromatic region is omitted.

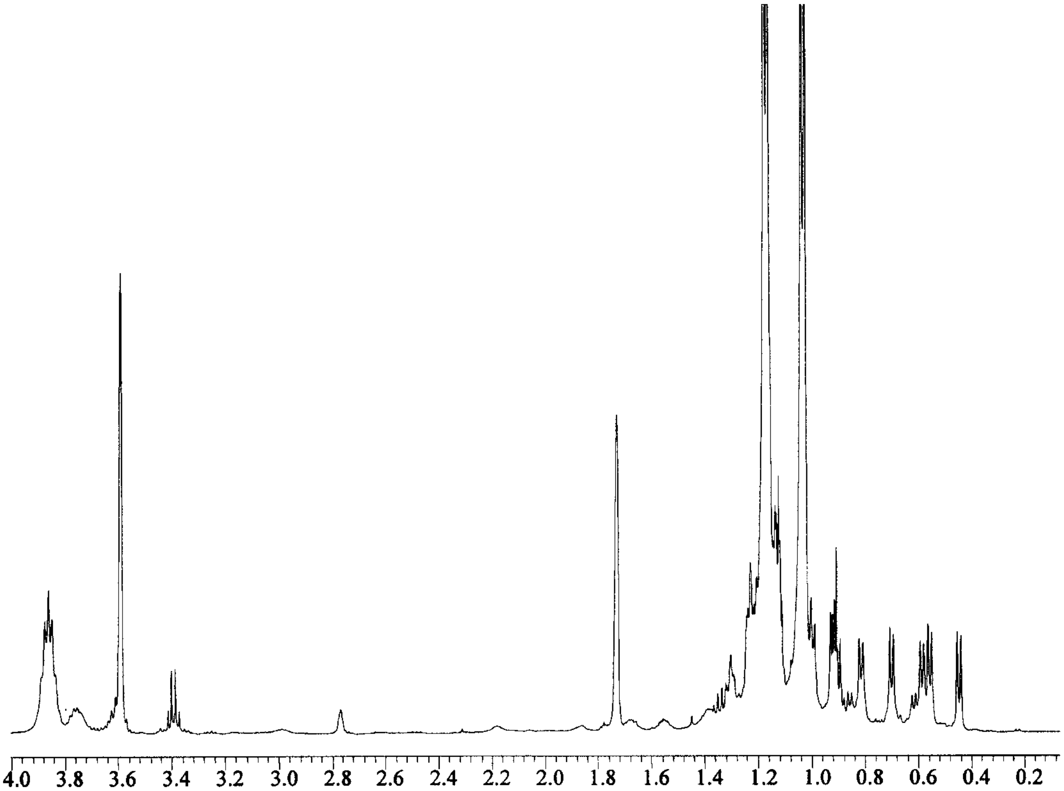

Figure 7. ^1H NMR spectrum of **1** in $[D_8]THF$ (500 MHz, 294 K). The aromatic region is omitted.

The spectrum shows only one signal for the methine protons (δ = 3.86 ppm) and two doublets for the methyl protons of the isopropyl substituents of the phenyl rings (1.16 and 1.03 ppm). These signals are assigned to (dpp-bian) $Mg(THF)_3$.[6c] The high field septet at δ = –0.44 ppm and the doublet at δ = 1.23 ppm reflect the presence of *i*Pr_2Mg in the solution. Thus, complex **3** being dissolved in THF dissociates into *i*Pr_2Mg and (dpp-bian)$Mg(THF)_3$. The ^1H NMR spectrum of **1** in $[D_{10}]Et_2O$ is not meaningful because of the paramagnetism of the complex, due to the presence of the dpp-bian radical anion. On dissolution of **1** in $[D_8]THF$ the color of the solution changes within minutes from cherry-red to green and the ^1H NMR spectrum indicates the absence of paramagnetic species (Figure 7).

The septet at δ = 3.86 ppm and the doublets at δ = 1.17 and 1.03 ppm prove that diamagnetic (dpp-bian)Mg-$(THF)_3$[6c] has been formed as a result of the elimination of *i*Pr radicals. As secondary products of the eliminated isopropyl radicals, the formation of propylene, propane, 2,3-dimethylbutane etc. is to be expected. Though certain amounts of these hydrocarbons are detected in the spectrum, the main reaction of the isopropyl radicals is the attack on THF molecules.

The ^1H-^1H COSY experiments revealed several cross peaks between pairs of doublets of low intensity (1.0–0.4 ppm) and broadened septets at relatively high fields (2.0–1.4 ppm). Thus, the doublets at 0.95 and 0.42, 0.81 and 0.59, and 0.70 and 0.55 ppm have cross peaks with septets at δ = 1.55, 1.67 and 1.39 ppm, respectively, and we assign these signals to *i*Pr substituted THF molecules. It is supposed that the coordinating strength of *i*Pr substituted THF molecules is somewhat higher than that of unsubstituted THF molecules and that the former will partly take the place of the THF ligands in (dpp-bian)$Mg(THF)_3$. The restricted rotation of the *i*Pr groups of magnesium coordinating *i*PrC_4H_7O ligands makes their methyl groups nonequivalent, thus giving rise to the doublets observed in the range 1.0–0.4 ppm.

Conclusions

The results of our investigations demonstrate that reductive elimination processes can be realized even with complexes of main group metals that are unable to change their oxidation state. This is accomplished when they are supported by the dpp-bian ligand, which may accept or deliver electrons.

Experimental Section

General Remarks: All manipulations were carried out in vacuo or under N_2 using Schlenk techniques. The solvents THF, Et_2O, hexane and toluene were distilled from sodium/benzophenone prior to use. The deuterated solvents [D$_8$]THF, and [D$_8$]toluene (Aldrich) were dried at ambient temperature over sodium/benzophenone and, just prior to use, condensed under vacuum into NMR tubes containing the compounds. The ^{1}H and ^{13}C NMR spectra were recorded with a Bruker ARX-400 and Bruker ARX-500 spectrometer. The UV/Vis spectra were recorded with a Perkin–Elmer Lambda 25 spectrometer.

(dpp-bian)(Mg-*i*Pr)(Et_2O) (1): A solution of (dpp-bian)Na was prepared by stirring dpp-bian (1.0 g, 2 mmol) and sodium (0.05 g, 2.17 mmol) in Et_2O (50 mL). After the sodium had dissolved completely, the solvent was evaporated in vacuo. Hexane (40 mL) was added to the remaining salt and the suspension that formed was stirred vigorously for 30 min. A 1 M solution of *i*PrMgCl (2.4 mL) in Et_2O was then added with vigorous stirring. Within a few seconds, the powdery (dpp-bian)Na dissolved and a cherry-red solution was formed which was filtered from NaCl and **2** and was then concentrated to 10 mL. Cooling of this solution to 0 °C yielded 0.47 g (37%) of **1** as deep-red crystals. M. p. 136–140 °C (decomp.). $C_{43}H_{57}MgN_2O$ (624.24): calcd. C 80.42, H 8.95; found C 80.33, H 8.96.

(dpp-bian)Mg(Et_2O)$_2$ (2): A 2 M solution of *i*PrMgCl in Et_2O (1.2 mL) was added to a stirred solution of (dpp-bian)Na prepared in situ from dpp-bian (1.0 g, 2 mmol) and sodium (0.05 g, 2.17 mmol) in Et_2O (50 mL). Within a few minutes the solution turned brown-green. The solvent was removed in vacuo and the solid dissolved in hot toluene. Cooling the solution to room temperature caused precipitation of **2** as yellowish-green crystals. Yield 1.1 g (72%) of **2**·(toluene). M. p. > 140 °C (decomp.). ^{1}H NMR spectrum (400 MHz, [D$_8$]THF, 20 °C): δ = 6.96 (d, 4 H, CH aromatic, ^3J = 7.3 Hz), 6.84 (t, 2 H, CH aromatic, ^3J = 7.3 Hz), 6.46 (d, 2 H, CH aromatic, ^3J = 6.8 Hz), 6.39 (dd, 2 H, CH aromatic, ^3J = 6.8 Hz), 5.37 (d, 2 H, CH aromatic, ^3J = 6.0 Hz), 3.86 (spt, 4 H, ^3J = 6.6 Hz), 3.34 (q, 8 H, *Et$_2$O*), 1.17 (d, 12 H, CH(C*H*$_3$)$_2$, ^3J = 6.8 Hz), 1.12 (t, 12 H, *Et$_2$O*), 1.03 (d, 12 H, CH(C*H*$_3$)$_2$, ^3J = 6.4 Hz). $C_{44}H_{60}MgN_2O_2 \cdot (C_7H_8)$ (765.4): C 80.03, H 8.95; found C 79.29, H 8.51.

(dpp-bian)(Mg-*i*Pr)$_2$(Et_2O) (3): A 2 M solution of *i*PrMgCl in Et_2O (2.4 mL) was added to a stirred solution of (dpp-bian)Na$_2$ prepared in situ from dpp-bian (1.0 g, 2 mmol) and sodium (0.1 g, 4.34 mmol) in Et_2O (50 mL). The color of the solution turned green and within seconds yellowish-green **2** precipitated. The solvent was removed in vacuo and the residual solid was treated with 40 mL of toluene. On heating to 70 °C the solid dissolved completely and the solution turned deep blue. The toluene was removed in vacuo and the residue was dissolved in hot hexane (80 mL). From the filtered solution, deep blue almost black crystals of **3** precipitated at 0 °C. Yield 0.85 g (60%). M. p. > 153 °C (decomp.). ^{1}H NMR spectrum (400 MHz, [D$_8$]THF, 20 °C): δ = 6.96 (d, 4 H, CH aromatic, ^3J = 7.5 Hz), 6.84 (t, 2 H, CH aromatic, ^3J = 7.5 Hz), 6.44 (d, 2 H, CH aromatic, ^3J = 8.1 Hz), 6.38 (dd, 2 H, CH aromatic, ^3J = 8.1 Hz), 5.36 (d, 2 H, CH aromatic, ^3J = 6.8 Hz), 3.86 (spt, 4 H, ^3J = 6.8 Hz), 3.39 (q, 8 H, *Et$_2$O*), 1.23 (d, 12 H, CH(C*H*$_3$)$_2$, ^3J = 7.8 Hz, *iPr$_2$Mg*), 1.17 (d, 12 H, CH(C*H*$_3$)$_2$, ^3J = 7.0 Hz), 1.12 (t, 12 H, *Et$_2$O*), 1.03 (d, 12 H, CH(C*H*$_3$)$_2$, ^3J = 6.8 Hz), –0.44 (spt, 2 H, ^3J = 7.8 Hz, *iPr$_2$Mg*). Anal calcd. (%) for $C_{46}H_{64}Mg_2N_2O$ (709.64): C 77.86, H 9.09; found C 77.25, H 8.97.

X-ray Crystallographic Study of 1–3: The crystal data and details of data collection are given in Table 1. The data for **1**–**3** were collected on a SMART CCD (graphite-monochromated Mo-K_α radiation, ω-scan technique, λ = 0.71073 Å). The structures were solved by direct methods using SHELXS-97[10] and were refined on F^2 using all reflections with SHELXL-97.[11] SADABS[12] was used to perform area-detector scaling and absorption corrections. The geometrical aspects of the structures were analyzed by using the PLATON program.[21] CCDC-250026 (for **1**), -250027 (for **2**) and -250028 (for **3**) contain the supplementary crystallographic data for this paper. These data can be obtained free of charge from The Cambridge Crystallographic Data Centre via www.ccdc.cam.ac.uk/data_request/cif.

Acknowledgments

This work was supported by the Alexander von Humboldt Stiftung (ILF), Russian Foundation for Basic Research (Grant No. 03-03-32246) and the Deutsche Forschungsgemeinschaft.

---

[1] "Le magnésium en chimie organique": V. O. F. Grignard, *Bull. Soc. Chim. Fr.* **1913**, *13*, 1–37.

[2] a) Ch. Elschenbroich, A. Salzer, *Organometallics*, 2nd ed., Wiley-VCH, Weinheim, **1992**; b) *Handbook of Grignard Reagents* (Eds.: G. S. Silverman, P. E. Rakita), Marcel Dekker: New York, **1996**; c) Grignard Reagents – New Developments (Ed.: H. G. Richey, Jr.), Wiley, Chichester, **2000**; d) P. Knochel, W. Dohle, N. Gommermann, F. F. Kneisel, F. Kopp, T. Korn, I. Sapountzis, V. A. Vu, *Angew. Chem. Int. Ed.* **2003**, *42*, 4302–4320; e) J. F. Garst, M. P. Soriaga, *Coord. Chem. Rev.* **2004**, *248*, 623–652.

[3] a) J. F. Coates, D. J. Ridley, *Biochem. Soc. Trans.* **1967**, 56–59; b) V. R. Magnuson, G. D. Stucky, *Inorg. Chem.* **1969**, *8*, 1427–1433; c) K. C. Yang, C. C. Chang, J. Y. Huang, C. C. Lin, G. H. Lee, Y. Wang, M. Y. Chiang, *J. Organomet. Chem.* **2002**, *648*, 176–187.

[4] a) R. Han, A. Looney, G. Parkin, *J. Am. Chem. Soc.* **1989**, *111*, 7276–7278; b) R. Han, G. Parkin, *J. Am. Chem. Soc.* **1990**, *112*, 3662–3663; c) R. Han, G. Parkin, *Organometallics* **1991**, *10*, 1010–1020; d) R. Han, G. Parkin, *J. Am. Chem. Soc.* **1992**, *114*, 748–757; e) P. Ghosh, G. Parkin, *Inorg. Chem.* **1996**, *35*, 1429–1430; f) M. H. Chisholm, N. W. Eilerts, J. C. Huffman, S. S. Iyer, M. Pacold, K. Phomphari, *J. Am. Chem. Soc.* **2000**, *122*, 11845–11854; g) J. L. Kisko, T. Fillebeen, T. Hascall, G. Parkin, *J. Organomet. Chem.* **2000**, *596*, 22–26.

[5] a) C. F. Caro, P. B. Hitchcock, M. F. Lappert, *J. Chem. Soc. Chem. Commun.* **1999**, 1433–1434; b) V. C. Gibson, J. A. Segal, A. J. P. White, D. J. Williams, *J. Am. Chem. Soc.* **2000**, *122*, 7120–7121; c) P. P. Bailey, S. T. Liddle, C. A. Morrison, S. Parsons, *Angew. Chem. Int. Ed.* **2001**, *40*, 4463–4466; d) M. H. Chisholm, J. C. Huffman, K. Phomphari, *J. Chem. Soc. Dalton Trans.* **2001**, 222–224; e) J. Prust, K. Most, I. Müller, E. Alexopoulos, A. Stasch, I. Usón, H. W. Roesky, *Z. Anorg. Allg. Chem.* **2001**, *627*, 2032–2037; f) P. P. Bailey, R. A. Coxall, C. M. Dick, S. Fabre, S. Parsons, *Organometallics* **2001**, *20*, 798–801; g) A. P. Dove, V. C. Gibson, E. L. Marshall, A. J. P. White, D. J. Williams, *J. Chem. Soc. Chem. Commun.* **2002**, 1208–1209; h) A. P. Dove, V. C. Gibson, P. Hormnirun, E. L. Marshall, J. A. Segal, A. J. P. White, D. J. Williams, *J. Chem. Soc. Dalton Trans.* **2003**, 3088–3097.

[6] a) I. L. Fedushkin, A. A. Skatova, V. A. Chudakova, G. K. Fukin, *Angew. Chem. Int. Ed.* **2003**, *42*, 3294–3298; b) I. L. Fedushkin, A. A. Skatova, V. A. Chudakova, V. K. Cherkasov, G. K. Fukin, M. A. Lopatin, *Eur. J. Inorg. Chem.* **2004**, 388–393; c) I. L. Fedushkin, A. A. Skatova, V. A. Chudakova, G. K. Fukin, S. Dechert, H. Schumann, *Eur. J. Inorg. Chem.* **2003**, 3336–3346; d) I. L. Fedushkin, V. A. Chudakova, A. A. Skatova, N. M. Khvoinova, Yu. A. Kurskii, T. A. Glukhova, G. K. Fukin, S. Dechert, M. Hummert, H. Schumann, *Z. Anorg. Allg. Chem.* **2004**, *630*, 501–507; e) I. L. Fedushkin, A. A. Skatova, A. N. Lukoyanov, V. A. Chudakova, S. Dechert, M. Hummert, H. Schumann, *Russ. Chem. Bull.* in press; f) I. L. Fedushkin, N. M. Khvoinova, A. Yu. Baurin, G. K. Fukin,

V. K. Cherkasov, M. P. Bubnov, *Inorg. Chem.* **2004**, *43*, 7807–7815; g) I. L. Fedushkin, A. A. Skatova, V. A. Chudakova, N. M. Khvoinova, A. Yu. Baurin, S. Dechert, M. Hummert, H. Schumann, *Organometallics* **2004**, *23* 3714–3718.

[7] a) M. W. van Laren, C. J. Elsevier, *Angew. Chem. Int. Ed.* **1999**, *38*, 3715–3717; b) R. van Belzen, H. Hoffmann, C. J. Elsevier, *Angew. Chem. Int. Ed. Engl.* **1997**, *36*, 1743–1745; c) G. A. Grasa, R. Singh, E. D. Stevens, S. P. Nolan, *J. Organomet. Chem.* **2003**, *687*, 269–279; d) A. Heumann, L. Giordano, A. Tenaglia, *Tetrahedron Letters* **2003**, *44*, 1515–1518; e) A. E. Cherian, E. B. Lobkovsky, G. W. Coates, *Chem. Commun.* **2003**, *20*, 2566–2567; f) M. D. Leatherman, S. A. Svejda, L. K. Johnson, M. Brookhart, *J. Am. Chem. Soc.* **2003**, *125*, 3068–3081; g) J. Kiesewetter, W. Kaminsky, *Chem. Eur. J.* **2003**, *9*, 1750–1758.

[8] a) I. L. Fedushkin, A. A. Skatova, V. K. Cherkasov, V. A. Chudakova, S. Dechert, M. Hummert, H. Schumann, *Chem. Eur. J.* **2003**, *9*, 5778–5783; b) I. L. Fedushkin, N. M. Khvoinova, A. A. Skatova, G. K. Fukin, *Angew. Chem. Int. Ed.* **2003**, *42*, 5223–5226; c) I. L. Fedushkin, A. A. Skatova, G. K. Fukin, M. Hummert, H. Schumann, *Eur. J. Inorg. Chem.*, in press; d) I. L. Fedushkin, A. A. Skatova, G. K. Fukin, M. Hummert, H. Schumann: these results will be published in a following paper.

[9] ORTEP3 for Windows: L. J. Farrugia, *J. Appl. Crystallogr.* **1997**, *30*, 565.

[10] G. M. Sheldrick, SHELXS-97 Program for the Solution of Crystal Structures; University of Göttingen, **1990**.

[11] G. M. Sheldrick, SHELXL-97 Program for the Refinement of Crystal Structures; University of Göttingen, **1997**.

[12] G. M. Sheldrick, SADABS Program for Empirical Absorption Correction of Area Detector Data; University of Göttingen, **1996**.

Received: November 23, 2004